IIETA International Information and Engineering Technology Association
Advancing the World of Information and Engineering

Journal Européen des Systèmes Automatisés
Vol. 59, No. 3, March, 2026, pp. 651-660
Journal homepage: http://iieta.org/journals/jesa

Enhancing Smart Grid Power System Using STATCOM Reactive Power Compensation Considering Electromagnetic Transients

Hasan Wahhab Salih Rabee[1*], Doaa Mohsin Majeed[2]

[1] Department of Electrical Technology, Najaf Technical Institute, Al-Furat Al-Awsat Technical University, Najaf 54001, Iraq
[2] School of Computer Science and Application Technology, Huazhong University of Science and Technology, Wuhan 430074, China

Corresponding Author Email: Hassan.wahhab.inj@atu.edu.iq

https://doi.org/10.18280/jesa.590309

Received: 14 January 2026
Revised: 13 March 2026
Accepted: 21 March 2026
Available online: 31 March 2026

Keywords:
STATCOM, smart grid, ultra-high voltage, photovoltaic, reactive power compensation, voltage stability, power quality, electromagnetic transient

ABSTRACT

The large-scale incorporation of photovoltaic (PV) generation stations at the ultra-high-voltage (UHV) transmission grid level introduces significant concerns related to voltage stability, dynamic reactive power support, and fault ride-through capability in the system. Conventional reactive power compensation methods often fail to provide fast dynamic voltage regulation during grid disturbances. Therefore, advanced dynamic compensation devices such as the Static Synchronous Compensator (STATCOM) have become essential for maintaining system stability. This article carries out a STATCOM investigation with a 500 kV smart grid-based PV source and conventional generation using electromagnetic transient (EMT) analysis. The STATCOM model was controlled using cascaded control loops using MATLAB/Simulink to investigate both the external voltage regulation response and the internal stress features of the device. The performance of the grid was tested and evaluated under different case studies, including voltage sag and swell events, switching of a 100 Mvar shunt capacitor bank, weak-grid conditions induced by line tripping, and single-line-to-ground (SLG) fault situations. Performance parameters in terms of the point of common coupling (PCC) voltage deviation, settling time, reactive power exchange, q-axis current tracking, and DC-link voltage ripple are obtained with STATCOM and without STATCOM. The obtained results show that the STATCOM is able to control the PCC voltage within very narrow limits (< 1.5%), with a setting time of 30 msec and better reactive power support without losing synchronization or overstressing internal components. The comparison shows that major improvements in voltage stability, dynamic damping, and fault ride-through capability are realized.

1. INTRODUCTION

The integration of photovoltaic (PV) generation in an ultra-high-voltage (UHV) transmission corridor is basically one of the main factors of the 500-kV grid, a future intelligent power system. Most of the time, the idea of solar PV generation will be taken for granted as the best method for the production of eco-friendly and sustainable energy. Still, the concept of solar PV is related to its variability, which incites rapid flow of voltage, imbalance of reactive power, and sometimes a local power system that is going by stable operation at the point of common coupling (PCC) stops abruptly [1].

Traditional reactive power compensation devices e.g., fixed capacitor banks or mechanically switched reactors, are not equipped with the necessary speed and flexibility to handle such fast dynamics. In the meantime, the Static Synchronous Compensator (STATCOM) is the perfect solution to all these problems and could be seen as one of the vital smart grid components that lead to the power system's reliability [2]. The efficient utilization of driving-voltage source converter technology together with cascaded control loops by the STATCOM gives sub-cycle reactive power support, therefore, the regulation of the PCC voltage, the system's stability improvement, and the smooth coordination between PV generation and the traditional source like gas turbines are achieved. Its importance becomes very clear in 500-kV grids, where the power transfer at a large scale can cause the effects of local disturbances to be seen at a considerable distance.

However, within the family of Flexible AC Transmission Systems (FACTS) controllers, the STATCOM is one of the leading solutions for dynamic reactive-power management, and it has been ranked as the most effective one. The voltage-source converter is connected to a DC link and controlled by cascaded control loops, phase lock loop (PLL) synchronization. Where the q-axis current control and outer voltage regulation with droop make the STATCOM very fast in its response. Thus, within a very short time, a fraction of the cycle then delivers the required reactive power or, if needed, will take away the excess from the system [3]. These features enable it to not only keep the voltage at the point of PCC stable during the occurrence of different disturbances and also to be a source of voltage for the weak grid in order to extend the fault ride-through (FRT) capability in accordance with the latest grid codes [4].

1.1 Previous woks

STATCOM devise compensation in utility grid was used to improve the voltage regulation, power quality improvement, and renewable integration. However, there is still a gap in research regarding a unified electromagnetic transient (EMT) framework assessment on how a ± 100-Mvar STATCOM at 60 Hz changes under various real-world disturbances, including programmed sags and swells, large shunt-capacitor insertion, line outages that weaken grid strength, and repeated unbalanced faults. The work [5] presented a comprehensive study of external performance and internal stress/complexity based on various operating scenarios of a 500-kV smart-grid system. The research concentrated on the isolated events scenarios or steady-state sizing without providing such lots of insightful information.

The authors in study [6] developed a comprehensive STATCOM model on a 500-kV three-bus system in conjunction with PV generation to fill the void in the literature. The EMT tested the device's capability under various conditions such as sag and swell, 100-Mvar capacitor switching, tripping of line 5, and double phase-to-ground faults. The control of smart grid techniques can combining the outer voltage regulation with the current/DC-link control that is at the core of the system for stability in case of grid disturbances [7]. The authors in study [8] proposed a coordinated controller method to select the transition point between capacitive and inductive modes as well as to stabilize the VAR balance that changes during the process of capacitor switching. Besides, the issue of the low SCR occurs because such as line tripping, conventional droop loops may lose their damping capability and may exhibit reduced stability margins. Therefore, the authors in study [9] proposed a virtual impedance/inductance augmentations method to improve the stability in the weak grids.

Furthermore, the literature provides comprehensive documentation of the behavior of the STATCOM and the voltage source converter (VSC) during the single-line-to-ground (SLG) faults. However, the focus is often on the design of the controller and the small-signal analysis, rather than the reproduction of EMT waveforms over several back-to-back disturbances along with the quantification of internal stresses such as dc-link voltage [10]. Also, Sizing studies can guide the adequacy of STATCOM rating for voltage regulation. Still, they mostly consider steady or single disturbance conditions, thus they do not show how a rating (e.g., ± 100 Mvar) can perform along with a compact set of realistic transmission events [11-15]. The study [11] presented an investigation of the most appropriate size of the STATCOM to improve voltage stability and FRT capability in fixed-speed wind farms connected to the utility grid. The authors firstly review the matters of voltage recovery from faults and regulation of voltage at a steady state occasion and point out the impact of the rating of the STATCOM on the issue. Moreover, simulation results support that properly sized STATCOMs are able to ensure safe voltage recovery post-fault and consequently minimal risk in disengaging of the generators. Regardless, the research [12] focused on the aspects of sizing and functional limits of the system while the performance of dynamic controllers is explored. Besides, the scope of the analysis is limited to the case of a wind farm and does not consider different types of disturbances or internal indicators of STATCOM stress, such as DC-link voltage variations. The paper [13] recommended the use of hydrogen fuel cells integrated with D-STATCOM technology for minimizing voltage sags and increasing the reliability of power systems.

The authors [14] presented different optimal STATCOM placement techniques in distribution networks with the objective of improving voltage profiles, reducing power losses, and enhancing system reliability. Various analytical, heuristic, and metaheuristic placement methods are classified and compared. The study provides a valuable overview of placement strategies and highlights key trends in distribution-level applications.

Ugwuanyi et al. [15] suggested a straightforward method for simultaneous enhancement of voltage and angle stability through the support of STATCOM. The solution proposed is kept simple and quite effortlessly possible to be implemented without the requirement of sophisticated control. The modeling outcomes reveal that both the voltage magnitude and phase stability have been quantitatively improved in the case of the conditions of selected operation. The article also fails to provide any treatment of internal converter dynamics and the transient stress behavior, which thereby limits the understanding of practical STATCOM operation. El Zoghby and Ramadan [16] improved the microgrid stability via optimally controlled STATCOMs for isolated microgrids. Upon application, it has been found that the load variations microgrid oscillation (voltage and frequency) can be effectively damped and the overall microgrid thus becomes more resilient to external disturbances and even load changes. However, a limitation with the study is that it only addresses isolated microgrids and does not explore grid-connected transmission systems.

Boghdady and Mohamed [17] proven that the use of a STATCOM-based reactive power compensation in conjunction with a modified maximum power point tracking (MPPT) strategy in a grid-connected PV system can improve the system performance. The primary objective of the proposed scheme is to stabilize voltage levels without compromising on PV power generation efficiency. The simulation outcomes reveal that the proposed method results in enhanced voltage regulation and power quality performance as compared to the traditional PV system employing only MPPT. The study [18] suggested a new control method for PV-STATCOM combined systems that would be able to regulate voltages and reactive power. Among other observations, the outcome indicates successful voltage regulation and notably improved grid support under different operating conditions. On the other hand, the control method created a higher level of SC complexity as compared to the conventional cascaded Proportional Integral (PI) controllers.

The research [19] focused on the potential application of virtual inertia delivered via STATCOM control for the improvement of power system dynamic stability. Moreover, through inertia emulation, the STATCOM is able to help stabilize frequency as well as voltage during transients thereby contributing to enhanced system stability. The studies based on simulations verify improved damping as well as superior response of the system after it has experienced a disturbance. However, the main intention is to inertia emulation and not the comprehensive aspect of voltage regulation. Effects related to reactive power saturation, converter stressing, and fault ride-through performance are not given the attention they deserve. Chakraborty et al. [20] focused at the control coordination between D-STATCOM and SVC devices based dynamic reactive power compensation in hybrid AC-DC grids. The

main purpose of the coordination strategy is to make the voltage more stable and thus alleviate the dynamic interferences between compensators. The results demonstrate superior voltage regulation compared to single-device solutions. However, the coordination increases control complexity and requires careful parameter tuning. The study is focused on medium-voltage AC-DC grids rather than UHV transmission systems. Nevertheless, the EMT-level analysis of the internal dynamics and fault ride-through behavior of the converter is limited.

1.2 Contributions

This study conducts an EMT-based analysis that is comprehensive for a ± 100 MVAR STATCOM at 60 Hz and tests it against four typical transmission-line disturbances, including voltage sag/swell, switching of a 100-MVAR capacitor bank, tripping of line 3 (weak grid condition), and repetitive SLG faults. The main contribution of this work is the control-oriented implementation and dynamic evaluation of a STATCOM-based reactive power compensation strategy under multiple EMT disturbances.

The other contributions of this paper include:

i. An EMT model of a ± 100 Mvar STATCOM connected to a 500 kV transmission node with significant PV penetration was developed, allowing very detailed time domain analyses beyond the conventional phasor based studies.

ii. The study considered the STATCOM device operation under a consecutive set of practical scenarios of the transmission level - voltage sag/swell, shunt capacitor-switching, line tripping for weak grid conditions and single line to ground faults repetition. Thus, it captured the real operating conditions of the modern smart grids.

iii. A comprehensive framework with and without STATCOM device was established to characterize voltage deviation limits, settling and recovery times, reactive power utilization and fault ride-through capability.

iv. The obtained results prove that the STATCOM can provide rapid reactive power support within its rated power even during severe and repeated faults, while maintaining the synchronization and keeping the currents limited. Thus, it fulfills the fault ride-through requirements of the UHV grids.

1.3 Rest of article

The reminder of the article is organized as follows: Section 2 presents the system model and methodology. Section 3 introduces the MATLAB simulation setup. Section 4 details the results and discussion. Section 5 provides the conclusion of the paper.

2. SYSTEM MODEL AND METHODOLOGY

2.1 System configuration

The suggested smart grid was evaluated by building a 500 kV 3-Bus transmission system in Figure 1. The suggested system include solar PV station (8500MW) and a ± 100 Mvar STATCOM using an EMT framework. The suggested system was modeled and tested using MATLAB/Simulink. However, the STATCOM system shown in Figure 2 using a synchronous dq-reference frame model that is aligned with the grid voltage by using a PLL method. The control system comprises three cascaded loops, the AC voltage regulator loop, the DC link voltage regulator loop, and the current regulator loop. The power exchange between the STATCOM and the grid is controlled by the AC voltage regulator loop. The DC-link voltage regulator loop restores the capacitor voltage equilibrium by the active current component id,ref. The two current references are given to the current regulator loop, which executes the current control at the setting of the fast tracking of id and iq. The resulting control signals are converted to the firing angles, which are the control inputs to the 48-pulse Voltage Source Inverter (VSI). This configuration enables the STATCOM to control the reactive power injection capable of voltage support and then improves the stability of the DC-link voltage.

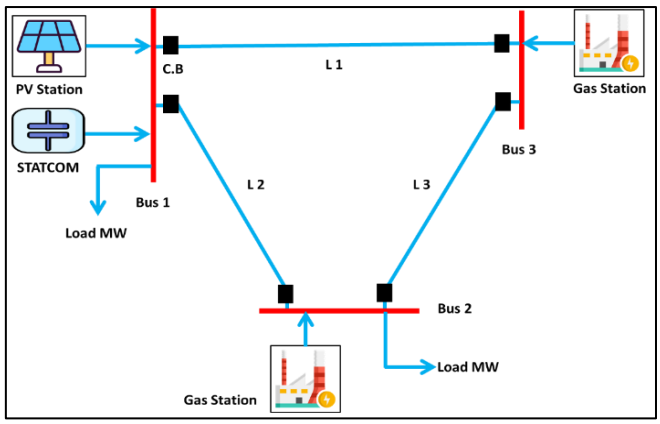

Figure 1. Typical single-line diagram of the 500-kV three-bus system

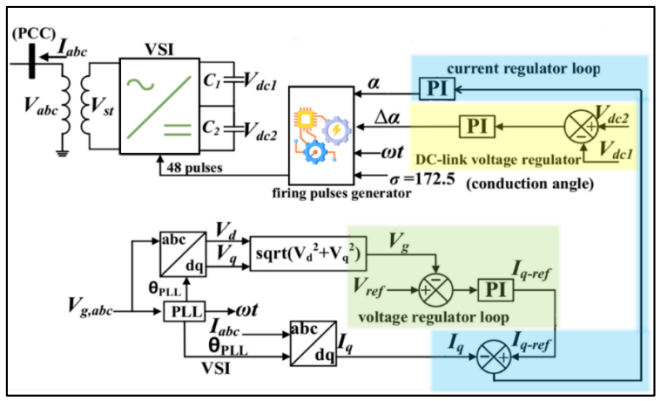

Figure 2. Block diagram of STATCOM control system

2.2 Modeling of STATCOM

The modeling of the STATCOM in the coordinate system of the rotating frame, which involves the exchange of electrical active and reactive powers. The behavior of converter current as well as the changes in the DC link, basically follows the generic VSC-based models as described in different studies [6, 7]. The device is represented as a converter with a voltage source on the DC-link side, a capacitor, a transformer reactance, and cascaded control loops. The converter voltage model depicts a voltage source with the ability to be controlled as in Eq. (1) [6]:

$$V_{conv} = m\, V_{dc}\, e^{j\,\alpha} \quad (1)$$

where, m is the modulation index, V_{dc} is the DC-link voltage, and α is the firing angle.

The active and reactive power flowed at the PCC are:

$$P = \frac{3}{2}\left(V_d\, i_d + V_q\, i_q\right) \quad (2)$$

$$Q = \frac{3}{2}\left(V_q\, i_d - V_d\, i_q\right) \quad (3)$$

Three-phase currents are represented in the dq-frame that is synchronized with the grid voltage angle θ are written as follows:

$$\begin{bmatrix} i_d \\ i_q \end{bmatrix} = \frac{2}{3}\begin{bmatrix} \cos\theta & \cos(\theta - \frac{2\pi}{3}) & \cos(\theta + \frac{2\pi}{3}) \\ -\sin\theta & -\sin(\theta - \frac{2\pi}{3}) & -\sin(\theta + \frac{2\pi}{3}) \end{bmatrix}\begin{bmatrix} i_a \\ i_b \\ i_c \end{bmatrix} \quad (4)$$

where, i_d is d-axis current, and i_q is the q-axis current. The error that comes from comparing the reference and measured voltages was written as follows.

The error that comes from comparing the reference and measured voltages was written as follows:

$$e_V = V_{ref} - V_{meas} \quad (5)$$

The reactive current reference is generated as:

$$i_{q,ref} = K_{pv}\, e_V + K_{iv} \int e_V\, dt - K_{droop}\, Q_{pu} \quad (6)$$

where, Q_{pu} is the reactive power of grid. The converter-side current dynamics of a current dynamics (Inner Loop) based Eqs. (7) and (8).

$$\frac{di_d}{dt} = \frac{1}{L}\left(v_d - R_{i_d} + \omega L_{i_q} - v_{conv,d}\right) \quad (7)$$

$$\frac{di_q}{dt} = \frac{1}{L}\left(v_q - R_{i_q} + \omega L_{i_d} - v_{conv,q}\right) \quad (8)$$

where, L_{i_q} and R_{i_d} are the reactance and resistance of the inverter's filter, ω is the fundamental grid frequency in rad/s. Thus, the DC-link capacitor dynamics are:

$$C\,\frac{dV_{dc}}{dt} = \frac{3}{2}\left(v_d\, i_d + v_q\, i_q\right) - \frac{V_{dc}}{R_{loss}} \quad (9)$$

The PI regulator stabilizes V_{dc} is written as follows:

$$i_{d,ref} = K_{pd}\,(V_{dc,ref} - V_{dc}) + K_{id}\int (V_{dc,ref} - V_{dc})\, dt \quad (10)$$

The grid angle can be found by setting the q-axis voltage to zero using PLL synchronization as follows:

$$e_{PLL} = v_q \quad (11)$$

$$\dot{\theta} = \omega = \omega_{nom} + K_p\, e_{PLL} + K_i \int e_{PLL}\, dt \quad (12)$$

3. SIMULATION SETUP

The proposed system with and without the STATCOM model has been developed and demonstrated by the MATLAB/Simulink software as shown in Figure 3.

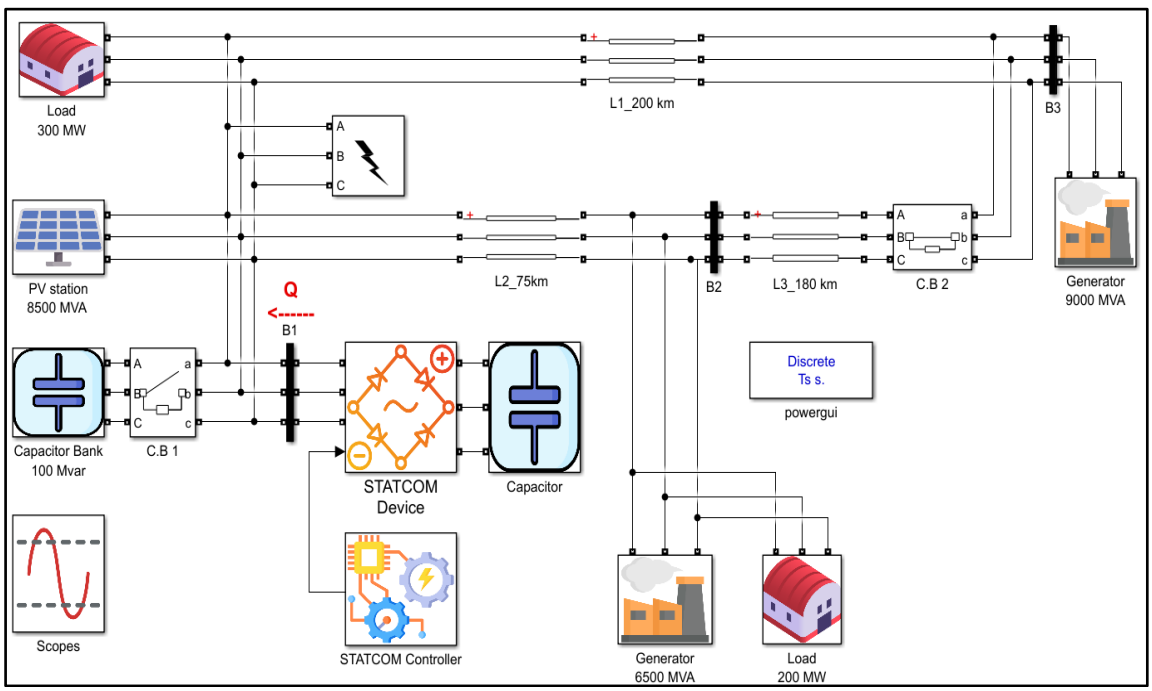

Figure 3. Simulink model of a smart grid, 3-Bus 500-kV with STATCOM device

In order to clarify the EMT modeling level adopted in this study, the STATCOM converter is depicted as a detailed EMT simulation framework developed in MATLAB/Simulink. The converter consists of a 48-pulse VSI, which is achieved by

combining two 24-pulse converter bridges through phase-shifting transformers. This setup drastically reduces low-order harmonics and enables the converter to reflect the dynamic interaction between the power electronic device and the transmission network during rapid transient events.

For this study, the converter model is mainly based on the EMT behavior of the power system, including voltage sag/swell, switching events, and fault conditions. Hence, the EMT simulation details the rapid changes of the STATCOM control system, the current response, and DC-link voltage during disturbances. Although the detailed switching of individual semiconductor devices is not explicitly modeled, the chosen 48-pulse equivalent model maintains the fundamental-frequency dynamics and the reactive power exchange features that largely govern the STATCOM response in transmission-level studies. Every controller gain is adjusted to get a rapid transient response as well as to keep the system stable. The main parameters that are used in the simulation are listed in Table 1. Moreover, the PV station with 8500 MW was added with two DGs as a voltage source that can be programmed. Thus, the PV system is connected to the DC/AC smart inverter to prove the AC voltage under changes with the radiation and the temperature. This addition depiction enables the effect of the intermittency of the clean energy supply to be visible in the network through the changes in the voltages that are pre-arranged, without the complete changes of the PV modules and converters. Table 2 shows system data parameters.

Table 1. Parameters of suggested grid

Parameter	Symbol	Value	Unit
Grid voltage (L-L, rms)	VLL	500	kV
Grid frequency	f	60	Hz
Line resistance	R	0.025	Ohm/Km
Line inductance	L	0.9	mH/
DC-link capacitance	Cdc	130	mF
DC-link reference voltage	Vdc,ref	20	kV
Converter type	VSI	48-pulse	–
Control sampling time	Ts	50	µs
PV station capacity	Ppv	8500	MW
Capacitor bank	Q	100	Mvar
Industrial load	PL	300	MW

Table 2. System data parameters

Parameter	Symbol	Value
Line lengths	L12	75 km
	L13	200 km
	L23	180 km
Transformer X/R ratios	X/R	01
PV power	Ppv	8500 MW
Generater power	G1	9000 MVA
Generater power	G2	6500 MVA
Base power	Sb	9000 MVA
Base voltage	Vb	500 KV

3.1 STATCOM controller implementation details

The STATCOM control parameter tuning was done through an iterative practical tuning procedure using time-domain simulations. Since the developed system is a large-scale transmission network that experiences various transient disturbances, it was quite challenging to get a closed-form analytical tuning solution for all cascaded control loops. That is why a well-structured trial-and-error tuning method was used to guarantee stable operation and a nice dynamic response. Initially, the inner current control loop was tuned to get a fast dynamic response. The controller PI gains set such that the current tracking bandwidth is much higher than that of the outer voltage control loops. This way, fast and accurate tracking of the reference currents idi and iqi are assured even during transient events like voltage sags and faults.

After that, the DC-link capacitor voltage control loop was tuned to provide stable voltage regulation of the capacitor without causing too many oscillations or interactions with the current controller. The controller gains were set stepwise until the DC-link voltage could smoothly recover after transient disturbances. Third, the AC voltage regulation loop was tuned to provide effective reactive power support and maintain the PCC voltage close to its reference value. The controller gains were selected to balance voltage regulation speed and system stability. During the tuning process, multiple simulation scenarios were used to verify controller robustness, including voltage sag/swell events, capacitor bank switching, transmission line tripping, and SLG faults. Table 3 reports the PI gains of the controllers. In addition, to clear the simulation results, Table 4 was added to show the test scenarios description.

Table 3. Reports the Proportional Integral (PI) gains of the controllers.

Parameter	Value
K_{pv}	5
K_{iv}	40
K_{droop}	0.03
K_{pd}	0.001
K_{id}	0.01
K_i	12
K_p	3000

Table 4. Test scenarios description

Scenarios	Event Time (s)	Duration (s)	Switching Condition
Voltage sag and swell	0.2, 0.4, 0.6, 0.8	0.2	Step change of source voltage (1.03 pu, 0.97 pu, 1.01 pu)
Capacitor Insertion	0.3	–	100 Mvar Capacitor bank connected at PCC
T.L tripping	0.2	0.4	Line-3 disconnected then reconnected
SLG fault	0.2 and 0.6	0.1	Single-line-to-ground (SLG) fault

4. RESULTS AND DISCUSSION

4.1 Evaluation and test scenarios

The response of the proposed system is validated against several representative scenarios that reflect realistic disturbances in smart grids with high renewable energy penetration. The scenarios aimed to test the steady-state voltage regulation, robustness, and internal stress behavior of the STATCOM control system under fast and severe network events. Under the first scenario, the STATCOM's dynamic voltage regulation performance is tested under renewable generation changes were tested by applying the programmed voltage sag and swell events at the grid side. The scenario 2 is

applied by considering a reactive power compensation (fixed bank of 100 Mvar capacitor). In scenario 3, a transmission line tripping is conducted in order to test the capability of the STATCOM to handle network topology changes.

In addition, the SLG is considered in last scenario to prove the effectiveness of the STATCOM control system.

This study uses a number of quantitative performance metrics to ensure the STATCOM performance. The maximum voltage deviation is the most significant change in the PCC voltage from its nominal value during the disturbance. The settling time is the time it takes for the PCC voltage to recover back to within ± 1% of its steady-state value after the disturbance. Recovery time is how long it takes for voltage to stabilize after the fault is cleared. Other performance indicators are the highest reactive power exchange, the highest q-axis current magnitude, and the highest peak-to-peak DC-link voltage ripple.

4.1.1 Scenario 1: Voltage sag and swell

In this sub-section, the voltage sag and swell events are applied to the system. However, the STATCOM is able to demonstrate highly beneficial dynamic voltage support through a rapid shift between the capacitive and inductive operating modes. As achieved, The PCC voltage was kept within a very narrow tolerance band, and the transient response was completed within a few fundamental cycles. The perfect following of the q-axis current reference and the low DC-link voltage ripple show that the cascaded control structure has enough bandwidth and damping to handle the quick changes that come with renewable generation intermittency. The obtained results without STATCOM was shown in Figure 4. As observed, the RMS positive-sequence voltage deviates from its reference quite noticeably. During an overvoltage period, the voltage rises to over 1.0 pu during under voltage events. No reactive current is generated, as the reactive power compensation is not available, and the Iq,ref changes largely in response to voltage fluctuations. The difference between the two indicates that the system can neither supply nor absorb reactive power, thereby leaving the PCC voltage unstable. Under no STATCOM, the solar station or the DG units pass through the transmission line without any diminution, thus the requirement for the dynamic VAR is still evident.

Figure 5 displays voltage variations that stress the STATCOM voltage regulator. The unit maintains phase synchronization with the grid where the converter phase voltage is superimposed on the grid voltage, while the STATCOM current is almost in quadrature, hence the power exchanged is mainly reactive. Because of the supply swelling to 1.03 pu, the controller turns the STATCOM to the inductive side. The reactive power changes smoothly to a negative value of − 50 Mvar. In addition, the positive-sequence voltage measured adjusts a little higher than the nominal (≈ 1.02 pu) instead of tracking the full swell. Thus, the reactive power is turned around to zero, no overshoot is noticed and the voltage returns to the reference.

Moreover, the STATCOM continues to inject a capacitive current similar in magnitude (+ 50 Mvar) which makes the voltage at the PCC with normal value. At all step changes, tracking of the reference of q-axis current is performed with very low steady-state error and even transient peaking of a very small magnitude. Their transition to the newly set operating point is done within several fundamental cycles (~65 msec), and the DC-link voltage has small, well-damped excursions. The STATCOM can absorb VARs during swells, injects VARs during sags, maintains the PCC voltage at the set point target while simultaneously, internal variables remain bounded.

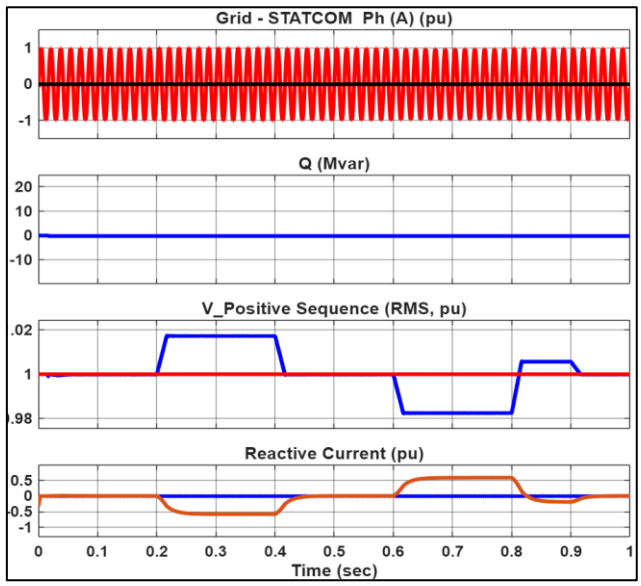

Figure 4. System response without STATCOM support

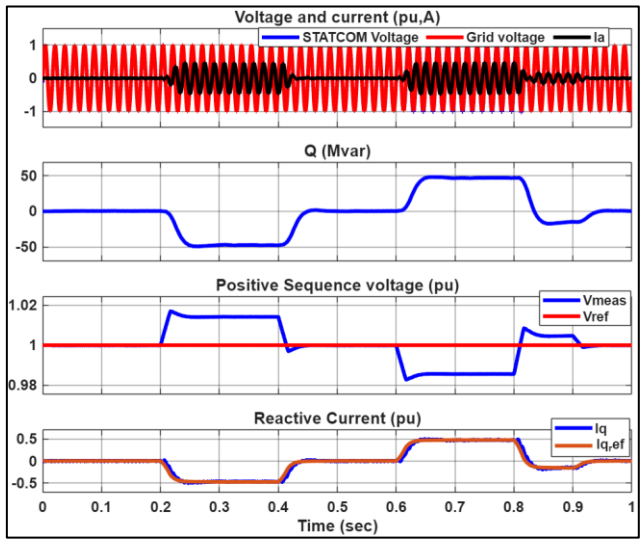

Figure 5. STATCOM response to voltage variation

Figure 6 displays the reactive current and STATCOM grid voltage waveforms. As observed in this figure, the tracking of the PLL is very accurate and the phase error is negligible. The converter current is mainly reactive and is kept very close to quadrature with the voltage. Thus, in the capacitive support, it leads the phase-A voltage by about 90° giving positive VARs that elevate the PCC voltage, at the step instants.

In Figure 7, the DC-link voltage is kept with its nominal level (20 kV) under different step changes. During a swell, the STATCOM moves to the inductive mode and thus takes a small amount of active power to the DC link with firing angles (1 − 1.5°). On the other hand, during the sag operation, the STATCOM operates in the capacitive mode, giving active power to the grid; α is slightly negative (−0.6 −0.8°), and the DC-link energy is adjusted before it is settled again. Thus, the voltage control loop is very strong and the system shows a controlled response without any drift.

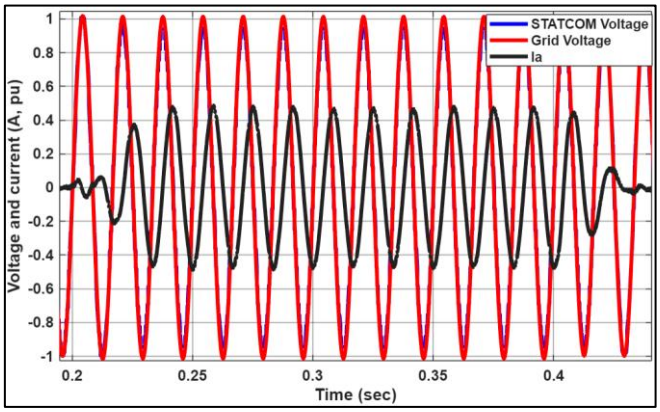

Figure 6. Reactive current and STATCOM-grid voltage waveforms

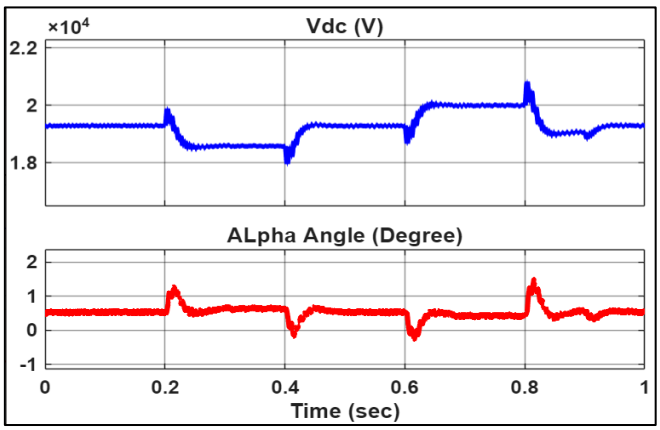

Figure 7. Response of the firing angle and DC voltage under scenario 1

4.1.2 Scenario 2: 100-Mvar shunt capacitor insertion

In this section, a 100 Mvar capacitor is added to the system. Figure 8 shows the STATCOM response. As shown, the STATCOM was very consistent with fixed reactive power compensation devices. When a surplus of reactive power was generated by the 100 Mvar capacitor bank, the STATCOM quickly took in the reactive power, and therefore the overvoltage caused by this was curtailed. The obtained settling time confirms that the STATCOM is able for mitigating the voltage disturbances caused by switching of the elements.

It can be inferred that the grid is supplying a surplus of reactive power. The STATCOM controller engages in inductive operation, causing the power to shift from positive to negative (approximately −40 to −60 Mvar). This action brings the voltage back to the reference level, remaining within a narrow band around 1 pu. The system's performance transitions from VARs to STATCOM when the VARs decrease (around 0.6 s), indicating that the compensator switches to capacitive support (+50 to +60 Mvar). Therefore, the voltage can be controlled when a small over-voltage occurrence at time 0.8 sec. The transitions in each case are very smooth, well-damped, and they manage to settle within a few 60-Hz cycles. In addition, the VARs, which are exchanged, remain well within the ± 00-Mvar limit that show the stable coordination between the fixed shunt bank and the dynamic compensator.

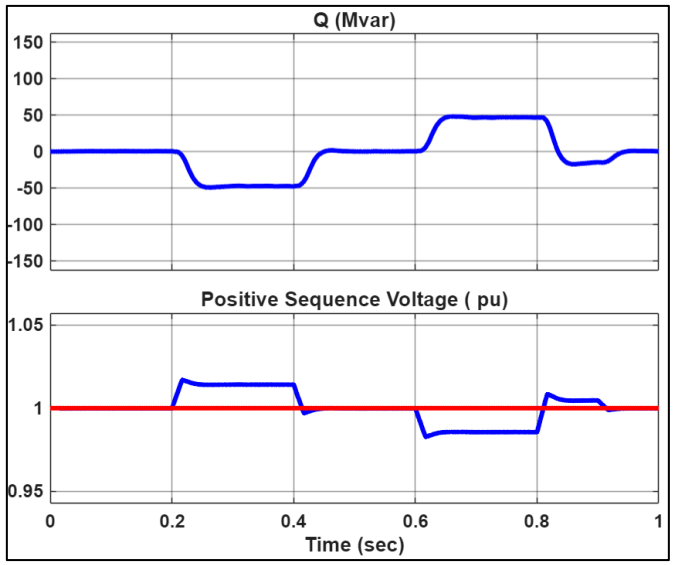

Figure 8. STATCOM response to 100-Mvar capacitor bank switching

4.1.3 Scenario 3: Tripping of transmission line (line No. 3)

Figure 9 represents the opening line No. 3 scenario at time of 0.2 s. The transmission line-tripping scenario represents a weak-grid condition that has a low short-circuit ratio and is more sensitive. As observed, the STATCOM is able to keep voltage regulation stable with a very small portion of its reactive power capacity. The small voltage variation and the quick voltage stabilization signify that the STATCOM has a sufficient reactive power. As observed in this figure, a transient value appears when the line is reconnected at time 0.6 s and the reactive output increased again. The voltage variation in both switching events is very small (≈ ± 0.5% around nominal). Thus, the obtained result indicates that the regulator keeps voltage support during grid changes and there is a significant margin for the ± 100-Mvar limit.

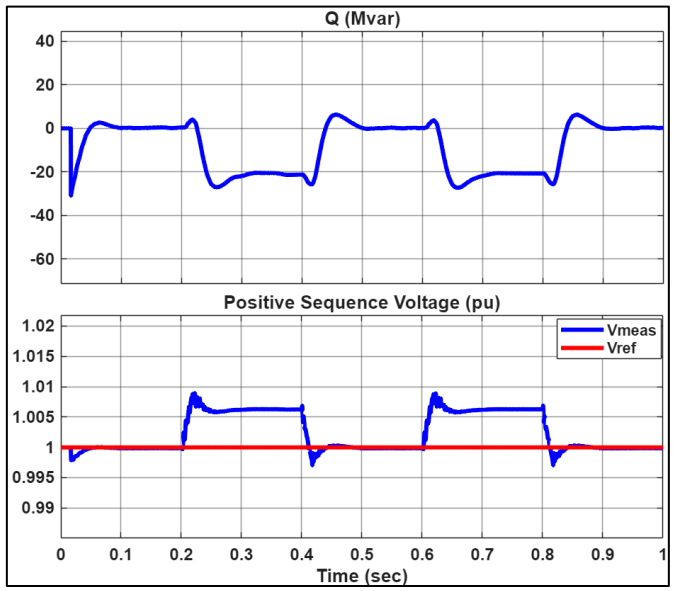

Figure 9. STATCOM reactive power and grid voltage at impact tripping line-3

4.1.4 Scenario 4: Single-line-to-ground fault

Figure 10 shows the SLG fault that is applied twice, at time 0.2 s and at time 0.6 s. Both faults cause the PCC positive-

sequence voltage to drop to roughly 0.72–0.75 pu while the STATCOM is still phase-locked to the grid. During the SLG fault events, the STATCOM is capable of delivering instant and quite substantial capacitive reactive power support with the rated limits. This performance confirms the excellent fault ride-through capability of the STATCOM and the robustness of the control system even when subjected repeatedly and severely to the disturbances. The sudden change in the q-axis current quickly prove the superior operation of the STATCOM. Moreover, the synchronization between the STATCOM and the grid is not disturbed, which means that the PLL has a very robust performance under unbalanced fault conditions. Once the fault is cleared, the STATCOM only for a moment consumes reactive power to prevent voltage overshoot, and after that, it goes back to its normal operation. The response of the control system being the same during the repeated fault event further confirms that the method is robust, reliable, and can be used again. This is an excellent demonstration of the control strategy being well-validated through the STATCOM's fault ride through capability in UHV grids.

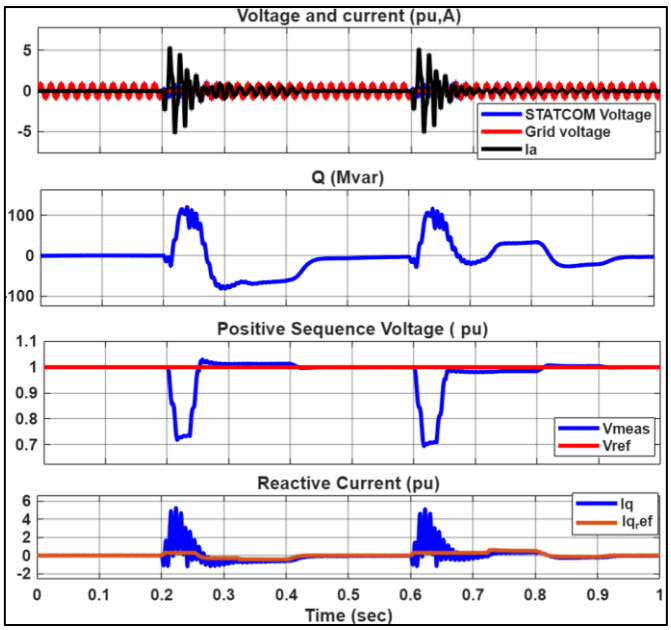

Figure 10. STATCOM response at single-line-to-ground (SLG) fault case

5. SYSTEM PERFORMANCE AND COMPARISON

In this study, the system without STATCOM is considered as the reference case representing a transmission network operating without fast dynamic reactive power compensation. This baseline allows a clear evaluation of the voltage regulation and fault ride-through improvements introduced by the STATCOM device.

To clear the novelty of the suggested system, comparative results of the suggested system with and without STATCOM under the applied tests are presented in Tables 5 and 6. As observed in this table, without the STATCOM, the PCC voltage is directly affected by variations in the source, switching of the capacitor, and changes in the network topology; as a result, there are significant voltage drops/heights, the system is not damped, and there is no reactive power support. The system does not have any voltage regulation capability that is dynamic; hence, there is no settling behavior observed. By connecting a STATCOM, the system changes significantly. During voltage sag and swell issues, the STATCOM dynamically supplies or withdraws reactive power (up to ± 50 Mvar) to maintain the PCC voltage within a tight ± 2% and achieve steady-state conditions within 50-70 msec.

The STATCOM in the capacitor switching case efficiently removes the extra reactance by working in the inductive mode. Hence, the overvoltage is limited to below 1.5%, and the coordination between the fixed and dynamic VAR devices is facilitated smoothly. Moreover, transmission line tripping weakens the grid, and under such conditions, the STATCOM reacts by absorbing a very small amount of reactive power, and at the same time, the voltage deviations are kept at below ± 0.5% with fast settling times. Thus, compensating reactive power was implemented and the STATCOM is very suitable for operation in low-SCR environments. However, during severe SLG faults, the STATCOM provides fast capacitive support up to its rated limit (100 Mvar), enabling rapid post-fault voltage recovery within 60–80 msec while maintaining synchronism and bounded current responses. In contrast, the system without STATCOM lacks fault ride-through capability and experiences deep voltage dips without controlled recovery.

Furthermore, the findings indicate that the main function of the STATCOM is serving to a steady-state voltage support device and providing fast dynamic voltage regulation. Result, an enhanced fault ride-through capability, and an improvement in the effectiveness of the system against weak-grid conditions and large disturbances. The inclusion of the STATCOM at 500 kV greatly improves voltage stability, power quality, and the capacity for hosting renewable energy sources. Finally, connecting STATCOM to the transmission system changes it from a passively reacting network to an actively regulated grid node that can support a high renewable penetration while maintaining voltage stability and operational security.

Table 5. Indices results of the suggested system with and without STATCOM

Scenario	Case	ΔV (%)	T_{st} (msec)	Q_{Peak} ($Mvar$)	$I_{q,Peak}$ ($p.u$)
Scenario 1	Without STATCOM	∓ 2.3	> 75	0	0
	With STATCOM	∓ 2	63	∓ 50	∓ 0.5
Scenario 2	Without STATCOM	$> +2$	> 68	100	-
	With STATCOM	∓ 1.5	55	$-60/+50$	-
Scenario 3	Without STATCOM	$> +1$	> 61	0	0
	With STATCOM	∓ 0.5	35	$-1\ 0$	-
Scenario 4	Without STATCOM	> 25	> 100	0	0
	With STATCOM	27	75	$+100$	4.5

Table 6. Stability comparison of the suggested system with and without STATCOM

Scenario	Case	Voltage Stability	Dynamic Stability
Scenario 1	Without STATCOM	Poor	Poor
	With STATCOM	Good	Stable
Scenario 2	Without STATCOM	Poor	Oscillatory
	With STATCOM	Excellent	Damped
Scenario 3	Without STATCOM	Poor	Low damping
	With STATCOM	Excellent	Robust
Scenario 4	Without STATCOM	Very Poor	Unprotected
	With STATCOM	Excellent	Stable

6. CONCLUSION AND FUTURE WORK

This article presented a detailed EMT-based evaluation of a ± 100 Mvar STATCOM connected to a 500 kV three-bus smart grid with high photovoltaic (PV) penetration. The investigation was aimed at determining the performance of the device both externally in voltage regulation and internally through stress indicators during transmission-level disturbances at realistic levels of each kind, such as voltage sag and swell, switching of shunt capacitor banks, tripping of transmission lines, and repetitive SLG faults. Simulation MATLAB results evidenced that, without using STATCOM, the voltage at the PCC would follow the disturbances in the network; thus, the resulting voltage deviations would be quite large, the voltage oscillations would be left un-damped, and no reactive power control would be possible. On the other hand, the STATCOM system proposed in this paper is able to supply quick and thus very effective dynamic reactive power compensation, which keeps the voltage level at the PCC within a narrow range of allowed values. During voltage variation tests, the STATCOM has been able to restrict voltage variations within ± 2% and has a voltage settling time of 50–70 msec. the suggested grid also tested under switching a capacitor bank, the combination of the fixed shunt elements and the STATCOM's operation. The scenario that had been prearranged was effective at lowering the overvoltage, with voltage deviations being approximately ± 1.5% and very smooth transient behavior. The STATCOM was handled the weak-grid conditions caused by the tripping of the transmission line; thus, it kept voltage variations below ± 0.5%. It supplied fast capacitive reactive power up to its rated limit during the most severe SLG fault conditions; thus, the post-fault voltage recovery was very quick (within 60–80 ms). The findings demonstrate that the device is able to maintain operation during faults and it has sufficient reactive power margin.

Numerous research directions can be considered for future work to build on the findings of this paper. First, the presented STATCOM model can be improved by the addition of energy storage devices, e.g., batteries or supercapacitors, to provide active power support besides reactive power compensation. Second, future work might be directed towards the development of adaptive or AI-based control such as model predictive control (MPC), fuzzy logic, or neural network controllers, to enhance the regulatory capability of the STATCOM in renewable generation and highly fluctuating grid conditions.

CONFLICT OF INTEREST

The authors declare no conflicts of interest.

DATA AND MODEL AVAILABILITY STATEMENT

The MATLAB/Simulink model and system parameters used in this study are available from the corresponding author upon reasonable request for research purposes.

REFERENCES

[1] Nazir, M.S., Ullah, H., Larik, N.A., Chu, Z., Tian, P., Sohail, H.M., Raute, R. (2024). Integrating FACTS technologies into renewable energy systems: Potential and challenges. International Journal of Ambient Energy, 45(1): 2409827. https://doi.org/10.1080/01430750.2024.2409827

[2] Diab, A.A.Z., Fawzy, I.Y., Elsawy, A.M., Abo El-Magd, A.G. (2025). Enhancing voltage stability in PV/Wind power systems with STATCOM utilizing fuzzy controller. Journal of Engineering Advances and Technologies for Sustainable Applications, 1(2): 32-53. https://doi.org/10.1109/REEPE63962.2025.10971104

[3] Sharma, S., Gupta, S., Zuhaib, M., Bhuria, V., Malik, H., Almutairi, A., Afthanorhan, A., Hossaini, M.A. (2023). A comprehensive review on STATCOM: Paradigm of modeling, control, stability, optimal location, integration, application, and installation. IEEE Access, 12: 2701-2729. https://doi.org/10.1109/ACCESS.2023.3345216

[4] Engelbrecht, T., Isaacs, A., Kynev, S., Matevosyan, J., Niemann, B., Owens, A.J., Singh, B., Grondona, A. (2023). Statcom technology evolution for tomorrow's grid: E-statcom, statcom with supercapacitor-based active power capability. IEEE Power and Energy Magazine, 21(2): 30-39. https://doi.org/10.1109/MPE.2022.3230969

[5] Chenchireddy, K., Kumar, V., Sreejyothi, K.R., Tejaswi, P. (2021). A review on D-STATCOM control techniques for power quality improvement in distribution. In 2021 5th International Conference on Electronics, Communication and Aerospace Technology (ICECA), Coimbatore, India, pp. 201-208. https://doi.org/10.1109/ICECA52323.2021.9676019

[6] Sadiq, R., Wang, Z., Chung, C.Y., Zhou, C., Wang, C. (2021). A review of STATCOM control for stability enhancement of power systems with wind/PV penetration: Existing research and future scope. International Transactions on Electrical Energy Systems, 31(11): e13079. https://doi.org/10.1002/2050-7038.13079

[7] Xu, Y., Li, F. (2014). Adaptive PI control of STATCOM for voltage regulation. IEEE Transactions on Power Delivery, 29(3): 1002-1011. https://doi.org/10.1109/TPWRD.2013.2291576

[8] Rafi, K.M., Prasad, P.V.N., Vithal, J.V.R. (2022). Coordinated control of DSTATCOM with switchable capacitor bank in a secondary radial distribution system for power factor improvement. Journal of Electrical

Systems and Information Technology, 9(1): 4. https://doi.org/10.1186/s43067-022-00044-3

[9] Wang, X., Feng, F., Peng, L., Xiao, P., Li, Z. (2025). Stability analysis and virtual inductance control for static synchronous compensators with voltage-droop support in weak grid. Electronics, 14(11): 2203. https://doi.org/10.3390/electronics14112203

[10] Hamdan, I., Ibrahim, A.M., Noureldeen, O. (2020). Modified STATCOM control strategy for fault ride-through capability enhancement of grid-connected PV/wind hybrid power system during voltage sag. SN Applied Sciences, 2(3): 364. https://doi.org/10.1007/s42452-020-2169-6

[11] Mahfouz, M.M.A., El-Sayed, M.A.H. (2014), Static synchronous compensator sizing for enhancement of fault ride-through capability and voltage stabilisation of fixed speed wind farms. IET Renewable Power Generation, 8: 1-9. https://doi.org/10.1049/iet-rpg.2012.0365

[12] Kilic, H., Asker, M.E., Haydaroglu, C. (2024). Enhancing power system reliability: Hydrogen fuel cell-integrated D-STATCOM for voltage sag mitigation. International Journal of Hydrogen Energy, 75: 557-566. https://doi.org/10.1016/j.ijhydene.2024.03.313

[13] Mosaad, M.I., Ramadan, H.S.M., Aljohani, M., El-Naggar, M.F., Ghoneim, S.S. (2021). Near-optimal PI controllers of STATCOM for efficient hybrid renewable power system. IEEE Access, 9: 34119-34130. https://doi.org/10.1109/ACCESS.2021.3058081

[14] Mumtahina, U., Alahakoon, S., Wolfs, P. (2023). A literature review on the optimal placement of static synchronous compensator (STATCOM) in distribution networks. Energies, 16(17): 6122. https://doi.org/10.3390/en16176122

[15] Ugwuanyi, N.S., Nwogu, O.A., Ozioko, I.O., Ekwue, A.O. (2024). An easy method for simultaneously enhancing power system voltage and angle stability using STATCOM. Scientific African, 25: e02248. https://doi.org/10.1016/j.sciaf.2024.e02248

[16] El Zoghby, H.M., Ramadan, H.S. (2022). Isolated microgrid stability reinforcement using optimally controlled STATCOM. Sustainable Energy Technologies and Assessments, 50: 101883. https://doi.org/10.1016/j.seta.2021.101883

[17] Boghdady, T.A., Mohamed, Y.A. (2023). Reactive power compensation using STATCOM in a PV grid connected system with a modified MPPT method. Ain Shams Engineering Journal, 14(8): 102060. https://doi.org/10.1016/j.asej.2022.102060

[18] Sonawane, A.J., Umarikar, A.C. (2023). Voltage and reactive power regulation with synchronverter-based control of PV-STATCOM. IEEE Access, 11: 52129-52140. https://doi.org/10.1109/ACCESS.2023.3276787

[19] Vetoshkin, L., Müller, Z. (2021). Dynamic stability improvement of power system by means of STATCOM with virtual inertia. IEEE Access, 9: 116105-116114. https://doi.org/10.1109/ACCESS.2021.3106236

[20] Chakraborty, S., Mukhopadhyay, S., Biswas, S.K. (2021). Coordination of D-STATCOM & SVC for dynamic VAR compensation and voltage stabilization of an AC grid interconnected to a DC microgrid. IEEE Transactions on Industry Applications, 58(1): 634-644. https://doi.org/10.1109/TIA.2021.3123264